

PCCP

Accepted Manuscript

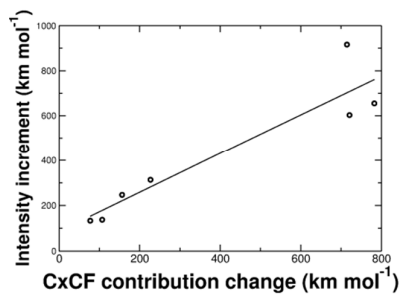


This is an *Accepted Manuscript*, which has been through the Royal Society of Chemistry peer review process and has been accepted for publication.

Accepted Manuscripts are published online shortly after acceptance, before technical editing, formatting and proof reading. Using this free service, authors can make their results available to the community, in citable form, before we publish the edited article. We will replace this *Accepted Manuscript* with the edited and formatted *Advance Article* as soon as it is available.

You can find more information about *Accepted Manuscripts* in the [Information for Authors](#).

Please note that technical editing may introduce minor changes to the text and/or graphics, which may alter content. The journal's standard [Terms & Conditions](#) and the [Ethical guidelines](#) still apply. In no event shall the Royal Society of Chemistry be held responsible for any errors or omissions in this *Accepted Manuscript* or any consequences arising from the use of any information it contains.



A semi-quantitative explanation for infrared intensity enhancements on hydrogen bonding is provided by a charge - charge flux interaction contribution.

An atom in molecules study of infrared intensity enhancements in fundamental donor stretching bands on hydrogen bond formation

Luiz A. Terrabuio,^a Wagner E. Richter,^b Arnaldo F. Silva,^b Roy E. Bruns,^b Roberto L.A. Haiduke^a

haiduke@iqsc.usp.br

^a Departamento de Química e Física Molecular, Instituto de Química de São Carlos, Universidade de São Paulo, CP 780, 13560-970, São Carlos, SP, Brazil

^b Instituto de Química, Universidade Estadual de Campinas, CP 6154, 13083-970, Campinas, SP, Brazil

Abstract

Vibrational modes ascribed to the stretching of X-H bonds from donor monomers (HX_{donor}) in complexes presenting hydrogen bonds ($\text{HF}\dots\text{HF}$, $\text{HCl}\dots\text{HCl}$, $\text{HCN}\dots\text{HCN}$, $\text{HNC}\dots\text{HNC}$, $\text{HCN}\dots\text{HF}$, $\text{HF}\dots\text{HCl}$ and $\text{H}_2\text{O}\dots\text{HF}$) exhibit large (from 4 to 7 times) infrared intensity increments during complexation according to CCSD/cc-pVQZ-mod calculations. These intensity increases are explained by the charge – charge flux – dipole flux (CCFDF) model based on multipoles from the Quantum Theory of Atoms in Molecules (QTAIM) as resulting from a reinforcing interaction between two contributions to the dipole moment derivatives with respect to the vibrational displacements: charge and charge flux. As such, variations that occur in their intensity cross terms on hydrogen bond formation correlate nicely with the intensity enhancements. These stretching modes of HX_{donor} bonds can be approximately modeled by sole

displacements of the positively charged hydrogens towards the acceptor terminal atom with concomitant electronic charge transfers in the opposite direction that are larger than those occurring for the H atom displacements of their isolated donor molecules. This analysis indicates that the charge-charge flux interaction reinforcement on H-bond complexation is associated with variations of atomic charge fluxes in both parent molecules and small electronic charge transfers between them. The QTAIM/CCFDF models also indicate that atomic dipole flux contributions do not play a significant role in the intensity enhancements.

Keywords: CCFDF, QTAIM, infrared intensities, vibrational modes, dimers, hydrogen bond

Introduction

Hydrogen-bonded complexes are interesting to study mainly because of their fundamental importance to the chemistry of life. They can be represented in a simplified way by X-H...Y, in which X is the donor unit atom directly bound to the bridge hydrogen while Y is an electronegative atom with lone electron pairs in the acceptor monomer. Many experimental measurements of geometrical parameters,¹⁻⁶ dipole moments,^{1,5,7-11} hydrogen bond dissociation energies^{2,12-17} and vibrational frequencies^{16,18-21} have been reported for the simple dimers investigated here.

Moreover, changes observed in the vibrational spectra of molecules undergoing dimerization have been studied for a long time. For instance, Dinur and Hagler evaluated the influence of atomic charge fluxes and variations in van der Waals parameters for hydrogen bond interactions and their consequences on structural changes and spectral shifts in the water dimer.²² Particular attention has been addressed to infrared intensity investigations of vibrational modes

in complexes linked by hydrogen bonds.²³⁻²⁶ Zilles and Person demonstrated that the polar tensor element associated with dipole moment derivatives along the hydrogen bond axis (O...H-O) due to bridge hydrogen displacement along this axis in the water dimer is significantly different from the equivalent one in an isolated molecule due mainly to charge flux according to the charge – charge flux – overlap (CCFO) partition,²⁷ with similar conclusions obtained for the HCN...HF dimer.²³ Yeo and Ford used atomic polar tensor invariants and Mulliken charges to also interpret intensity variations on hydrogen bonding.²⁴ Exchange and charge transfer effects are cited as important quantities in these studies.²⁵ Another recent investigation with the Equilibrium Charge - Charge Flux (ECCF) model also reinforced the importance of charge fluxes to these intensity enhancements of X-H stretching modes on hydrogen bonding.²⁶ In addition, effects of basis set superposition errors (BSSEs) on intensities have also been determined for the HF...HF dimer.²⁸ This work suggested that infrared intensities obtained at the self-consistent field (SCF) level should only be slightly affected by BSSEs.

The CCFO partition model²⁷ for dipole moment derivatives has been normally based on Mulliken charges and fluxes calculated from them. However, a new investigation has pointed out that charge fluxes derived from the Mulliken formalism do not show a clear convergence pattern with basis set size increments and may lead to results in large disagreement with chemical expectations based on well-established physical arguments.²⁹ Another alternative partition is represented by the charge – charge flux – overlap modified (CCFOM) model, in which charge and charge flux are defined directly from polar tensor elements.³⁰ However, CCFOM leads to dominant charge fluxes for stretchings in LiH and NaH, which are inconsistent with the harpoon mechanism determined for such ionic molecules.²⁹

Recently, dipole moment derivatives are being analyzed by the charge – charge flux – dipole flux (CCFDF) model,³¹ which employs changes in charges and atomic dipoles from the Quantum Theory of Atoms in Molecules (QTAIM),^{32,33} to investigate infrared intensities.³⁴ Thus, the contribution from variations in anisotropies of atomic electron densities during vibrations (atomic dipole fluxes), an important aspect of the QTAIM formalism, is fully taken into account in this infrared intensity partition. Hence, the QTAIM/CCFDF model provides an alternative tool to understand the origins of variations in infrared intensities of fundamental bands. In fact, this model was employed to evaluate infrared intensities of C-H stretchings in polycyclic aromatic hydrocarbons.³⁵ The dipole moment derivatives during the displacement of the a^{th} atom are expressed in this model as

$$p_{zz}^a = \frac{\partial p_z}{\partial z_a} = q_a + \sum_i z_i \frac{\partial q_i}{\partial z_a} + \sum_i \frac{\partial m_{i,z}}{\partial z_a} \quad \text{and} \quad (1)$$

$$p_{xz}^a = \frac{\partial p_x}{\partial z_a} = \sum_i x_i \frac{\partial q_i}{\partial z_a} + \sum_i \frac{\partial m_{i,x}}{\partial z_a} \quad , \quad (2)$$

in which q and m represent charges and total atomic dipole (sum of electronic and nuclear contributions) components, respectively, and i is an atomic index.

These derivatives can also be converted to normal coordinates (Q_α),^{36,37}

$$\frac{\partial p_z}{\partial Q_\alpha} = \sum_i q_i \frac{\partial z_i}{\partial Q_\alpha} + \sum_i z_i \frac{\partial q_i}{\partial Q_\alpha} + \sum_i \frac{\partial m_{i,z}}{\partial Q_\alpha} = \left(\frac{\partial p_z}{\partial Q_\alpha} \right)_C + \left(\frac{\partial p_z}{\partial Q_\alpha} \right)_{CF} + \left(\frac{\partial p_z}{\partial Q_\alpha} \right)_{DF} \quad , \quad (3)$$

in which the three terms that arise are respectively known as charge (C), charge flux (CF) and atomic dipole flux (DF) contributions to dipole moment derivatives. Moreover, infrared fundamental intensities (A_α),

$$A_{\alpha} = \frac{N\pi}{3c^2} \left(\frac{\partial \bar{p}}{\partial Q_{\alpha}} \right)^2, \quad (4)$$

are finally decomposed in several terms according to the QTAIM/CCFDF treatment³⁷

$$A_{\alpha} = \frac{N\pi}{3c^2} \left[\left(\frac{\partial \bar{p}}{\partial Q_{\alpha}} \right)_C^2 + \left(\frac{\partial \bar{p}}{\partial Q_{\alpha}} \right)_{CF}^2 + \left(\frac{\partial \bar{p}}{\partial Q_{\alpha}} \right)_{DF}^2 + 2 \left(\frac{\partial \bar{p}}{\partial Q_{\alpha}} \right)_C \left(\frac{\partial \bar{p}}{\partial Q_{\alpha}} \right)_{CF} + 2 \left(\frac{\partial \bar{p}}{\partial Q_{\alpha}} \right)_C \left(\frac{\partial \bar{p}}{\partial Q_{\alpha}} \right)_{DF} + 2 \left(\frac{\partial \bar{p}}{\partial Q_{\alpha}} \right)_{CF} \left(\frac{\partial \bar{p}}{\partial Q_{\alpha}} \right)_{DF} \right] = A_{\alpha}^C + A_{\alpha}^{CF} + A_{\alpha}^{DF} + A_{\alpha}^{C \times CF} + A_{\alpha}^{C \times DF} + A_{\alpha}^{CF \times DF}, \quad (5)$$

meaning that the intensity is a sum of individual contributions from charge, charge flux and dipole flux as well as their cross terms. See also that eqs. (4) and (5) imply scalar products of the vectors present.

In addition, QTAIM has also been used to provide important characterization criteria for hydrogen bonding interactions.³⁸ Correlations between some of these QTAIM quantities and an experimental parameter of hydrogen bond basicity were also investigated for Platts.³⁹ The details of hydrogen bond energetics within the QTAIM formalism have also been the focus of an interesting study that showed the crucial role of mutual penetration between acid and base molecules.⁴⁰ As a result of this mutual penetration, the dipolar polarization of the bridge hydrogen decreases upon hydrogen bonding.³⁸ Another energetic partition based on similar arguments also shed some light into the covalent/electrostatic view of hydrogen bonding interactions, discussing the charge transfers observed under formation of these dimers.⁴¹

This work is concerned with the study of variations in dipole moment derivatives and infrared intensities of X-H stretching modes ascribed to the donor molecule due to hydrogen bond formation by means of the recently developed QTAIM/CCFDF partition model.³¹ We selected a series of simple dimers and complexes to facilitate the data analysis: HF...HF,

HCl...HCl, HCN...HCN, HNC...HNC, HCN...HF, HF...HCl and H₂O...HF. Electronic structure calculations were performed at the CCSD/cc-pVQZ-mod level, in an attempt to minimize significantly BSSEs and to include high-order electron correlation corrections to provide one of the most advanced treatments ever tried for these dimers.

Computational details

Calculations in this work were performed with the Gaussian 03 package.⁴² This software assumes a harmonic potential so its intensity estimates do not include corrections for anharmonicity. However anharmonic perturbations on vibrational intensities are of the second order (for diatomics involving a product of the cubic potential energy term by the curvature of the dipole moment function at equilibrium geometry) contrary to the expectedly more important first order corrections to harmonic frequencies.⁴³ The CCSD method was chosen along with a modified version of cc-pVQZ sets, labeled as cc-pVQZ-mod. These modified sets are obtained by removing the function with the largest angular momentum of each atom from the original cc-pVQZ^{44,45} to reduce the computational demand. Some calculations to evaluate the need for diffuse functions were also done with aug-cc-pVTZ sets.^{44,45} All quantities are determined from generalized densities, which are the correct densities associated with post-Hartree-Fock electron correlation treatments. AIMALL⁴⁶ was employed to obtain QTAIM multipoles. The results obtained at equilibrium geometries for the density Lagrangian or, as also called, the Laplacian function, $L[\Omega]$, which provides an evaluation of integration accuracy of QTAIM quantities, are within indicated ranges (absolute values between 1.3×10^{-5} and 1.2×10^{-4} a.u. for hydrogens and from 2.4×10^{-7} to 5.5×10^{-5} for the other atoms).⁴⁷ In addition, basis set superposition errors were

evaluated by means of the counterpoise method.^{48,49} Numerical two-point estimates of charge and atomic dipole derivatives are obtained by 0.01 Å atomic displacements from equilibrium structures. Linear monomers and dimers were displaced along the Cartesian z axis while the X-H bond in donor molecules of the remaining dimers is also aligned along this axis.

Results and discussion

Molecular properties at equilibrium geometries

Table S1 presents some geometrical equilibrium data obtained for monomers and dimers according to our CCSD/cc-pVQZ-mod treatment. The agreement with available experimental data^{1-6,50,51} is satisfactory. One can notice that the theoretical X-H bond length of donor monomers is always enlarged due to dimerization (from 0.002 to 0.013 Å). Equilibrium dissociation energies (D_e) of hydrogen bonds are given in Table 1. These values are corrected for basis set superposition errors (BSSEs) and such corrections are also reported in this table. First, one can see that the CCSD/cc-pVQZ-mod BSSEs are all small because of the considerable size of basis sets employed in this work with the H₂O...HF dimer presenting the largest BSSE, 0.63 kcal mol⁻¹. Nevertheless, these BSSEs account for a contribution that reaches only 14 % of corrected D_e values at the extreme case. Moreover, the agreement with experimental values^{2,12-17} is nice, with deviations smaller than 10 % except for HCl...HCl and also for one of the available experimental results of H₂O...HF. Validation CCSD/aug-cc-pVTZ calculations furnished larger BSSEs in almost all cases except for H₂O...HF and these errors can now be as large as 22% of the corrected D_e values.

Moreover, Table 2 shows the molecular dipole moments. The agreement between CCSD/cc-pVQZ-mod and experimental values^{1,5,7-11,50} is satisfactory with the largest deviations (around 0.4 Debye) observed in heterodimers. The data obtained in this work also indicate that the dimers exhibit larger dipole moments than those derived from the simple vectorial addition of monomer dipoles by 0.3 to 1.1 Debye. The dipole moments estimated in the CCSD/aug-cc-pVTZ validation calculations are almost the same as those of our preferred treatment level, with differences of up to 0.06 Debye.

The results from QTAIM, Table S2, show that the bridge hydrogen atoms are more positively charged in the complexes than in their respective isolated molecules (from 0.02 to 0.06 e). These findings are in close agreement with previous studies that involved Mulliken charges of several hydrogen-bonded complexes^{23,24} and NBO results for the water dimer.⁵² On the other hand, the ECCF model indicates the opposite tendency for these atoms²⁶ and this disagreement is probably caused by the ECCF assumption that molecular dipole moments are completely explained by atomic charges only. In addition, the X atom receives some electronic charge on complexation (between -0.03 and -0.05 e) according to our study while the opposite occurs for the hydrogen atoms of acceptor units (from 0.01 to 0.03 e). QTAIM values (Table S2) also point to small electronic charge transfers from acceptor to donor units occurring on hydrogen bond formation, which varies between 0.004 and 0.030 e . NBO analyses and the ECCF model also confirm that hydrogen bonding is accompanied by an electronic charge transfer from acceptor to donor molecules.^{26,52} These charge changes predicted by QTAIM are in line with the molecular dipole moment strengthening that was observed on dimerization.

Infrared intensities

Furthermore, Tables 3 and 4 contain theoretical and the available experimental values of vibrational frequencies^{16,18-21,50,53} and fundamental infrared intensities^{54,55} for the monomers and H-bond complexes. The most striking feature caused by complexation on hydrogen bond formation is a remarkable intensity enhancement for the X-H bond stretching mode of the donor molecule (HX_{donor}), which varies from 4 to 7 times the monomer intensity corresponding to absolute increments between 132 and 911 km mol^{-1} according to our CCSD/cc-pVQZ-mod calculations. In addition, the intensity of the stretching modes for the X-H bonds of the acceptor molecules (HX_{acceptor}) also shows an increase on dimerization, although the absolute differences are much less expressive. Experimental measurements indicated that the HX_{donor} band is approximately two to three times more intense than the HX_{acceptor} vibration in HF...HF and HCl...HCl dimers,^{19,56} while our CCSD/cc-pVQZ-mod results provide slightly larger intensity ratios (3.45 for HF...HF and 3.60 for HCl...HCl). Moreover, as expected, the frequency of the HX_{donor} stretching mode decreases because of the intermolecular bond formation, which is customarily interpreted as resulting from bond weakening. Another work found in the literature also shows the vibrational frequencies and infrared intensities for the HF...HF dimer as obtained in CCSD(T) calculations with some triple- and quadruple-zeta basis sets.¹⁸ The individual frequencies for HF stretching modes from the largest basis set of this article are slightly different from ours but the variations on dimerization are nearly the same. Moreover, these CCSD(T) infrared intensities are almost equal to the ones found by us. The validation data from the aug-cc-pVTZ sets also do not provide significant differences. QTAIM/CCFDF intensities from CCSD/cc-pVQZ-mod calculations, also in Tables 3 and 4, are in excellent agreement with their

reference results (deviations up to 9 km mol^{-1}), confirming the numerical quality of the CCFDF parameters.

The analysis described in eq. (5) was used in order to seek an interpretation for the intensity enhancements of the HX_{donor} stretching modes due to hydrogen bonding. Table 5 contains the QTAIM/CCFDF contributions to the infrared intensities of the monomers and complexes. Some features noticed before in a group of mostly organic molecules can also be detected in our results.³⁷ First, the predominantly negative values for the charge flux – dipole flux interaction contribution ($A_{\alpha}^{CF \times DF}$) are expected because a negative correlation between both of these contributions to dipole moment derivatives was detected in previous studies with the QTAIM/CCFDF model.³¹ HNC is the only exception presenting a small positive $A_{\alpha}^{CF \times DF}$ contribution (11 km mol^{-1}). Another consequence of this negative correlation is that two cross terms involving charge with charge flux and dipole flux ($A_{\alpha}^{C \times CF}$ and $A_{\alpha}^{C \times DF}$) all show opposite signs (See Table 5) except once again for HNC, where the absolute values of these contributions are small. Finally, this negative correlation also implies that the charge flux and atomic dipole flux contributions to the intensities (A_{α}^{CF} and A_{α}^{DF}) should be approximately proportional, as was indeed observed in our results. This is apparent on inspection of the values in Table 5. For example, HCN and its dimer have the largest charge flux and dipole flux intensity contributions whereas HNC and its dimer have some of the lowest values. This means that increases in the intramolecular charge transfer during vibrations are accompanied by increased polarizations of the electron density in the opposite direction, an idea closely related to the known counter polarization concept presented by Bader for electronic charge distributions in equilibrium geometries.⁵⁷ Since negative correlations between charge flux and dipole flux have been found

for many vibrational motions studied with the QTAIM/CCFDF model³¹ the counter polarization concept seems relevant for small amplitude distortions.

Table 6 contains the variations in each contribution to the infrared intensities shown in eq. (5) caused by hydrogen bond formation. The first aspect to be discussed is that the contributions ascribed to charge and dipole flux are relatively unaffected on dimerization (from -72 to 102 km mol⁻¹). Accordingly, the cross term between both these quantities, $A_{\alpha}^{C \times DF}$, is also of minor importance in explaining the intensity enhancements due to hydrogen bonding (differences between -96 and 143 km mol⁻¹ on complexation). Hence, the most relevant variations are observed in those contributions that depend directly on the electronic charge flux phenomenon, A_{α}^{CF} , $A_{\alpha}^{C \times CF}$ and $A_{\alpha}^{CF \times DF}$. The sum of these three quantities associated with charge flux and their interactions (CF terms), also given in Table 6, explains almost completely the increments in intensities caused by hydrogen bond formation except for one dimer, HF...HF, in which case a nearly exact cancellation occurs for charge flux related terms. In addition, the changes in A_{α}^{CF} and $A_{\alpha}^{CF \times DF}$ contributions may be positive or negative. Interestingly, variations in A_{α}^{CF} are only negative for complexes with HF as donor monomer while the opposite is observed for $A_{\alpha}^{CF \times DF}$, which only presents negative differences for the other dimers. Since their correlation coefficient (R) is -0.96 a partial cancellation exists between the A_{α}^{CF} and $A_{\alpha}^{CF \times DF}$ values in Table 6. However, the interaction between charge and charge flux, $A_{\alpha}^{C \times CF}$, always contributes to enhancements in infrared intensities during complexation and it may constitute a general feature of these hydrogen-bonded complexes. Finally, we investigate if this last contribution alone is able to explain most of the strengthening observed during hydrogen bonding. Hence, a graph of these intensity increments against changes found in the $A_{\alpha}^{C \times CF}$ cross

interaction is shown in Fig. 1. A linear correlation coefficient of 0.93 is found along with a slope equal to 0.862. This R value implies a semi-quantitative explanation for the intensity enhancement on hydrogen bonding by means of the $A_{\alpha}^{C \times CF}$ term.

Atomic contributions to the infrared fundamental intensities

As Eq. (4) shows, the square root of infrared fundamental intensities is a measurement of absolute values for dipole moment derivatives with respect to normal coordinates. Thus, considering that the HX_{donor} bond is positioned along the Cartesian z axis and assuming that the normal mode ascribed to the stretching of this particular bond can be simply represented by a displacement of the donor hydrogen atom along this axis as supported by our vibrational calculations, these derivatives in terms of normal coordinates should be nearly proportional to p_{zz}^{Hd} , a polar tensor element of the donor hydrogen atom. This proportionality is in fact supported by our results for HX_{donor} stretchings (see Table S3). Furthermore, we also arrived at similar $\Delta(A^{C \times CF})$ contributions to the ones seen in Table 6 by means of the p_{zz}^{Hd} values (see Table S4). We now proceed to the analysis of p_{zz}^{Hd} elements instead of normal modes themselves since additional complications associated with the motion of other atoms are avoided (normal mode variations on dimerization and atomic displacements in different directions for monomers and their respective nonlinear dimers), yielding a simpler comparison and interpretation of atomic displacements for the monomers and dimers. Moreover, as seen in eq. (1), p_{zz}^{Hd} elements can be partitioned into charge, charge flux and dipole flux contributions. Hence, we can take charge changes during the displacement of the hydrogen atom of the donor molecule to investigate how the electronic charge flows in this vibrational mode. This strategy was also adopted by Zilles and

Person.²³ Our results indicate that the most relevant charge derivatives are those of this hydrogen and the X atom, except for the HNC...HNC dimer. In this case, the carbon charge of the donor monomer is predominantly affected by hydrogen displacement. Consistently, as the HX_{donor} bonds in the complexes increase, this already positively charged hydrogen (between 0.25 and 0.78 e) tends to lose even more electronic charge (from 0.02 to 0.2 $e \text{ \AA}^{-1}$) while the X atom receives more electronic charge (between -0.02 and -0.3 $e \text{ \AA}^{-1}$) when compared with the results for the respective displacements in their isolated molecules (the ECCF model points to the opposite tendency for hydrogen in many cases²⁶). Nitrogen and carbon, respectively, in the HCN and HNC dimer donors also gain some extra electronic charge with respect to equivalent displacements in the isolated molecules (around -0.05 $e \text{ \AA}^{-1}$). Thus, this is in line with positive differences found in the $A_{\alpha}^{C \times CF}$ cross term due to hydrogen bond formation (Table 6 and Fig. 1). Another similar effect that contributes to the reinforcement in $A_{\alpha}^{C \times CF}$ terms on complexation occurs in the acceptor monomer because of induced charge changes originating from the displacement of the bridge hydrogen, but it appears to be less important. In addition, there are some small electronic charge transfers from acceptor to donor molecules (from 0.01 to 0.09 $e \text{ \AA}^{-1}$) as hydrogen moves towards the Y atom of the acceptor molecule. Such transfers also contribute to the increments found for the $A_{\alpha}^{C \times CF}$ interaction on hydrogen bonding. Similar charge transfers are observed in the ECCF model.²⁶

Eq. (1) is not adequate to analyze the contributions of individual atomic charge fluxes to these p_z^{Hd} elements of donor monomers because some of the individual terms are not translationally invariant. However, since the sum of charge derivatives of all atoms on displacement of the bridge hydrogen must be zero ($\sum \partial q_i / \partial z_{\text{Hd}} = 0$), one can derive an equation with only translationally invariant terms,

$$p_{zz}^{Hd} = \frac{\partial p_z}{\partial z_{Hd}} = q_{Hd} + z_{XHd} \frac{\partial q_X}{\partial z_{Hd}} + z_{YHd} \frac{\partial q_Y}{\partial z_{Hd}} + \frac{\partial m_{X,z}}{\partial z_{Hd}} + \frac{\partial m_{Y,z}}{\partial z_{Hd}} + \frac{\partial m_{Hd,z}}{\partial z_{Hd}} + \text{other atomic terms} , \quad (6)$$

in which $z_{ab}=z_a-z_b$. This equation can be written in a more physically appealing way as

$$p_{zz}^{Hd} = \frac{\partial p_z}{\partial z_{Hd}} = q_{Hd} - R_{XHd} \frac{\partial q_X}{\partial z_{Hd}} + R_{YHd} \frac{\partial q_Y}{\partial z_{Hd}} + \frac{\partial m_{X,z}}{\partial z_{Hd}} + \frac{\partial m_{Y,z}}{\partial z_{Hd}} + \frac{\partial m_{Hd,z}}{\partial z_{Hd}} + \text{other atomic terms} , \quad (7)$$

for the coordinate system used here with the HX donor bond aligned along the z-axis and the X atom positioned in the negative direction. The second term in Eq. (7) represents electronic charge transfer to the X atom. It has a negative sign because the transfer is in the negative direction. It is a product of the charge derivative times the HX_{donor} bond length and could be interpreted as the quantity of charge transferred from H_d to X times the distance associated with the transfer. The third term is positive and describes charge transfer in the opposite direction from the hydrogen donor atom to the acceptor Y atom, where R_{YHd} is the projection of the hydrogen bond length on the z-axis (absolute value). There is one analogous charge flux term as well as a derivative of its atomic dipole for each of the other atoms in the complex, whose terms are implicit in Eq. (7).

Table 7 contains the differences observed in the terms of eq. (7) as given by the QTAIM/CCPDF analysis on hydrogen bonding (individual values for monomers and dimers are in Table S5). The charge term (q_{Hd}) increases slightly on complexation and presents only a small contribution to the concomitant enhancements of this p_{zz}^{Hd} element, which will result only in minor infrared intensity increments. The polarization change for the bridge hydrogen ($\partial m_{Hd,z}/\partial z_{Hd}$) also becomes slightly more positive due to the hydrogen bond formation, but this effect on p_{zz}^{Hd} variations is almost entirely cancelled by contributions of polarization variations encountered for the X atom ($\partial m_{X,z}/\partial z_{Hd}$). In addition, the dipole flux of atom Y ($\partial m_{Y,z}/\partial z_{Hd}$) may increase or decrease p_{zz}^{Hd} depending on the complex being studied. Finally, the charge flux for

the X atom, $(\partial q_X/\partial z_{Hd})(R_{XHd})$, changes on complexation, which results in substantial increments of p_z^{Hd} , while the opposite usually occurs, but to a smaller extent, for the Y atom, $(\partial q_Y/\partial z_{Hd})(R_{YHd})$. Furthermore the values in Table 7 clearly provide evidence of large charge flux (CF) contributions to the infrared intensity enhancements from the other atoms on hydrogen bonding.

Table 8 presents a different grouping of terms in eq. (6), which allows discrimination of the three main sources of atomic charge flux changes on complexation (individual values for monomers and dimers are in Table S6). As mentioned in the previous paragraph, one can see that increments in the bridge hydrogen charge and polarization changes on complexation are in general the least important factors to explain the concomitant increases in p_z^{Hd} , which only leads to minor infrared intensity enhancements. The most important source of charge flux contributions to the p_z^{Hd} change on hydrogen bonding is certainly that associated with all the atoms of the donor monomer $(\sum_{i \in d} z_{iHd} \partial q_i / \partial z_{Hd})$, which varies from 0.06 to 0.25 e and results in an average of 0.16 e . Next, we observe that the charge flux from acceptor to donor units $(\sum_{i \in a} z_{YHd} \partial q_i / \partial z_{Hd})$ is the second most relevant factor to these p_z^{Hd} variations, ranging from 0.02 to 0.19 e , with an average of 0.10 e . The last atomic charge flux source, which is associated with charge changes on the acceptor monomer $(\sum_{i \in a} z_{iY} \partial q_i / \partial z_{Hd})$, responds for p_z^{Hd} variations due to hydrogen bonding from -0.01 to 0.18 e , thus resulting in an average of only 0.07 e . Consequently, according to our study, the sum of these three effects is the fundamental reason for the infrared intensity enhancement of HX_{donor} stretchings caused by hydrogen bonding. This work confirms, in general lines, the findings from Zilles and Person,²³ which is surprising considering the known limitations of SCF/4-31G calculations and Mulliken charges. In spite of some observed divergences, our study also agrees with the main conclusions from the ECCF

model such as the non-local character of the charge fluxes in the stretching modes of these systems.²⁶ Furthermore the insignificance of the atomic dipole flux contributions confirms the validity of their absence in models explaining intensity enhancements even though their contributions are important to accurately describe the intensities of both the monomers and dimers individually.

Conclusions

Our results show that the main cause for the remarkable enhancement observed in infrared intensities of fundamental bands associated with the X-H stretching of donor units due to hydrogen bond formation, when compared to their isolated monomers, is a reinforcing interaction between charge and charge flux contributions, $A_{\alpha}^{C \times CF}$. The charge contribution is ascribed to dipole moment variations which occur when one or more charged atoms are displaced from their equilibrium positions. Charge flux effects result in dipole moment changes because of electronic charge transfers between atoms of a molecule during a vibration. We demonstrated that these increments found for the intensities of the X-H donor modes correlate nicely with variations occurring in the $A_{\alpha}^{C \times CF}$ interaction term on hydrogen bonding.

The changes in the $A_{\alpha}^{C \times CF}$ term during X-H donor bonds enlargements occur because more relevant electronic charge fluxes are observed in the direction towards X in the presence of a hydrogen bond than those found in the isolated donor molecules. In this case, the bridge hydrogen tends to become even more positively charged in the dimer while the opposite occurs to the X atom. There are also some concomitant electronic charge transfers from acceptor to

donor units that play a secondary role in the intensity strengthening. Charge fluxes in acceptor monomers also are calculated to have some enhancement effect, although minor.

Thus, the main aspects seen here are in line with interpretations based on the ECCF model, although some divergences are observed.²⁶ Our work also agrees with the general conclusions drawn by Zilles and Person for a displacement of the bridge hydrogen atom alone in the water dimer.²³ However, a more complete analysis of the water dimer should take into account normal mode changes on dimerization.⁵⁸

Acknowledgements

The authors thank FAPESP (Fundação de Amparo à Pesquisa do Estado de São Paulo) (grant numbers 2010/18743-1 and 2009-09678-1) and CNPq (Conselho Nacional de Desenvolvimento Científico e Tecnológico (grant number 300544/2009-0) for financial support. L.A.T. also thanks FAPESP for a graduate fellowship (grant number 2011/02807-3). W.E.R. and A.F.S. thank CNPq for graduate student fellowships (140711/2013-9 and 140916/2011-3) and R.E.B. thanks CNPq for a research fellowship.

Supporting Information

Additional tables containing geometry parameters, QTAIM charges, infrared intensity and polar tensor increment data on dimerization.

Table 1: Equilibrium dissociation energies of hydrogen bonds obtained from CCSD/aug-cc-pVTZ and CCSD/cc-pVQZ-mod calculations corrected for basis set superposition errors and from experiment (kcal mol^{-1}).

Dimers	CCSD/aug-cc-pVTZ ^a	CCSD/cc-pVQZ-mod ^a	Exp
HF...HF	4.15 (0.48)	4.16 (0.47)	4.56 ± 0.29^{12}
HCl...HCl	1.54 (0.34)	1.45 (0.13)	2.27 ± 0.25^{12} ; 1.98^2
HCN...HCN	4.46 (0.57)	4.43 (0.19)	4.40^{13}
HNC...HNC	6.64 (0.65)	6.63 (0.25)	
HCN...HF	6.95 (0.56)	6.69 (0.46)	6.88 ± 0.11^{14} ; 6.12 ± 0.38^{15}
HF...HCl	2.40 (0.36)	2.37 (0.33)	
H ₂ O...HF	7.81 (0.49)	7.79 (0.63)	7.2 ± 2^{16} ; 10.2 ± 0.2^{17}

^a Values between parenthesis are basis set superposition errors.

Table 2: Dipole moment values obtained from CCSD/aug-cc-pVTZ and CCSD/cc-pVQZ-mod calculations along with experimental data (Debye).

System	CCSD/aug-cc-pVTZ	CCSD/cc-pVQZ-mod	Exp
HF	1.81	1.82	1.83^{50}
HCl	1.10	1.13	1.11^{50}
HCN	3.05	3.03	2.99^{50}
HNC	3.09	3.09	3.05^{50}
H ₂ O	1.86	1.90	1.85^{50}
HF...HF	3.28	3.28	$2.99^{1,7}$
HCl...HCl	1.76	1.79	1.5 ± 0.1^8
HCN...HCN	6.88	6.83	6.55^9
HNC...HNC	7.30	7.29	
HCN...HF	5.82	5.76	5.61^{10}
HF...HCl	2.77	2.77	2.41^5
H ₂ O...HF	4.49	4.50	4.07 ± 0.01^{11}

Table 3: Vibrational frequencies (cm^{-1}) and fundamental infrared intensities (km mol^{-1}) obtained from CCSD/aug-cc-pVTZ and CCSD/cc-pVQZ-mod calculations and QTAIM multipoles along with experimental values for the monomers.^a

Monomers	Mode	CCSD/aug-cc-pVTZ		CCSD/cc-pVQZ-mod		QTAIM/CCFDF ^b	Exp	
		Freq	Int	Freq	Int	Int	Freq	Int
HF	ν_1	4173	110	4199	108	108	4138 ⁵⁰	77.5 ⁵⁴
HCl	ν_1	3017	36	3025	37	37	2991 ⁵⁰	33.2 ⁵⁴
HCN	ν_1	3463	67	3467	66	66	3311 ⁵⁰	59.3 ⁵⁴
	ν_2	2173	0.6	2185	0.6	0.6	2097 ⁵⁰	0.2 ⁵⁴
	ν_3^c	744	35	749	35	35	712 ⁵⁰	50.2 ⁵⁴
HNC	ν_1	3847	263	3852	262	262	3653 ⁵³	108; 182 ⁵⁵
	ν_2	2103	63	2111	58	58	2024 ⁵³	29 ⁵⁵
	ν_3^c	475	131	464	135	135	464 ⁵³	157 ⁵⁵
H ₂ O	ν_1	3853	4.6	3883	4.9	4.9	3657 ⁵⁰	2.9 ⁵⁴
	ν_2	1659	73	1673	70	70	1595 ⁵⁰	62.5 ⁵⁴
	ν_3	3959	59	3987	53	53	3756 ⁵⁰	41.7 ⁵⁴

^a Theoretical values refer to the harmonic approximation;

^b From CCSD/cc-pVQZ-mod calculations;

^c The intensity shown is associated with only one of these two degenerate modes.

Table 4: Vibrational frequencies (cm^{-1}) and fundamental infrared intensities (km mol^{-1}) obtained from CCSD/aug-cc-pVTZ and CCSD/cc-pVQZ-mod calculations and QTAIM multipoles along with experimental values for some stretching modes of the complexes.^a

Dimers		CCSD/aug-cc-pVTZ		CCSD/cc-pVQZ-mod		QTAIM/CCFDF ^b	Exp
Y...HX	Attribution	Freq	Int	Freq	Int	Int	Freq
HF...HF	HF _{donor}	4070	429	4103	421	421	3868 ¹⁸
	HF _{acceptor}	4138	125	4164	122	121	3931 ¹⁸
	F...H	155	15	159	15	17	125;128 ¹⁸
HCl...HCl	HCl _{donor}	2977	186	2989	169	171	2857,2839 ^{19,c}
	HCl _{acceptor}	3003	45	3012	47	47	2880 ¹⁹
	Cl...H	70	2	62	4	4	
HCN...HCN	HC _{donor}	3400	333	3394	312	313	3202 ²⁰
	HC _{acceptor}	3450	59	3462	67	67	3303 ²⁰
	CN _{donor}	2168	18	2180	17	17	2092 ²⁰
	CN _{acceptor}	2188	8	2199	7	7	2113 ²⁰
	N...H	119	2	116	2	2	119 ²⁰
HNC...HNC	HN _{donor}	3609	1205	3616	1173	1178	
	HN _{acceptor}	3835	287	3840	287	287	
	NC _{donor}	2105	8	2114	7	7	
	NC _{acceptor}	2145	57	2153	53	53	
	C...H	146	3	144	3	3	
HCN...HF	HF _{donor}	3942	819	3993	764	763	3716 ²¹
	HC _{acceptor}	3452	88	3466	86	86	3310 ²¹
	CN _{acceptor}	2202	7	2212	7	7	2121 ²¹
	N...H	182	4	179	4	4	168 ²¹
HF...HCl	HCl _{donor}	2985	178	2992	180	175	
	HF _{acceptor}	4151	143	4175	142	142	
	F...H	95	28	96	11	12	
H ₂ O...HF	HF _{donor}	3906	737	3943	702	711	3608 ¹⁶
	HO(sym) _{acceptor}	3865	55	3897	56	56	
	HO(asym) _{acceptor}	3970	104	4002	99	99	
	O...H	222	5	227	4	4	180 ¹⁶

^a Theoretical values refer to the harmonic approximation;

^b From CCSD/cc-pVQZ-mod calculations;

^c These two values occur due to tunneling splitting.

Table 5: QTAIM/CCFDF contributions to fundamental infrared intensities of X-H stretching modes (km mol^{-1}) in monomers and dimers obtained from CCSD/cc-pVQZ-mod calculations.

Systems	Attribution	QTAIM/ CCFDF ^a						Total
		A ^C	A ^{CF}	A ^{DF}	A ^{C×CF}	A ^{C×DF}	A ^{CF×DF}	
HF	HF	577.2	487.0	71.2	-1060.3	405.4	-372.4	108.0
HCl	HCl	65.3	178.0	234.4	215.6	-247.5	-408.5	37.4
HCN	HC	0.6	1217.4	758.4	52.2	-41.2	-1921.8	65.6
HNC	HN	443.9	3.5	9.1	-78.7	-127.0	11.3	262.1
HF...HF	HF _{donor}	675.5	257.1	111.6	-833.4	548.8	-338.4	421.1
HCl...HCl	HCl _{donor}	71.2	301.9	162.8	293.0	-215.4	-442.9	170.6
HCN...HCN	HC _{donor}	5.4	1996.7	860.8	208.6	-136.9	-2622.1	312.5
HNC...HNC	HN _{donor}	534.4	189.1	6.5	635.8	-117.7	-70.0	1178.2
HCN...HF	HF _{donor}	616.5	31.3	70.4	-277.8	416.7	-93.9	763.2
HF...HCl	HCl _{donor}	91.3	285.2	175.8	322.6	-253.1	-446.9	174.7
H ₂ O...HF	HF _{donor}	552.8	52.1	107.6	-339.5	487.8	-149.8	711.1

^a See eq. (5).

Table 6: Variations in QTAIM/CCFDF contributions to the infrared intensities of X-H stretching modes (km mol^{-1}) due to dimerization obtained from CCSD/cc-pVQZ-mod calculations.

Dimers		QTAIM/ CCFDF ^a							Tot
Y...HX	Attrib.	$\Delta(A^C)$	$\Delta(A^{CF})$	$\Delta(A^{DF})$	$\Delta(A^{C \times CF})$	$\Delta(A^{C \times DF})$	$\Delta(A^{CF \times DF})$	$\Delta(A^{CF \text{ terms}})$	
HF...HF	HF _{donor}	98.3	-229.9	40.4	226.9	143.3	34.1	31.1	313.1
HCl...HCl	HCl _{donor}	5.9	123.9	-71.6	77.4	32.1	-34.4	166.9	133.3
HCN...HCN	HC _{donor}	4.9	779.3	102.4	156.4	-95.8	-700.3	235.4	246.9
HNC...HNC	HN _{donor}	90.5	185.6	-2.6	714.6	9.3	-81.2	818.9	916.1
HCN...HF	HF _{donor}	39.3	-455.7	-0.8	782.6	11.2	278.6	605.4	655.2
HF...HCl	HCl _{donor}	26.0	107.2	-58.6	107.0	-5.7	-38.4	175.7	137.4
H ₂ O...HF	HF _{donor}	-24.4	-434.9	36.4	720.9	82.4	222.7	508.7	603.1

^a $\Delta(A^I) = A^I(\text{dimer}) - A^I(\text{monomer})$.

Table 7: Variations on hydrogen bonding for atomic terms of the QTAIM/CCFDF analysis of the polar tensor elements (e) associated with parallel dipole moment derivatives for displacements of the bridge hydrogen along the X-H axis from CCSD/cc-pVQZ-mod calculations.^a

Differences ^b	Δq_{Hd}	$\Delta \left(-R_{xHd} \frac{\partial q_x}{\partial z_{Hd}} \right)$	$\Delta \left(R_{yHd} \frac{\partial q_y}{\partial z_{Hd}} \right)$	$\Delta \left(\frac{\partial m_{Hd,z}}{\partial z_{Hd}} \right)$	$\Delta \left(\frac{\partial m_{x,z}}{\partial z_{Hd}} \right)$	$\Delta \left(\frac{\partial m_{y,z}}{\partial z_{Hd}} \right)$	Other atoms		Tot
							$\Delta(CF)$	$\Delta(DF)$	
HF...HF	0.021	0.157	-0.018	0.059	-0.056	0.049	0.079	0.002	0.294
HCl...HCl	0.018	0.063	0.023	0.025	0.006	0.037	0.048	-0.001	0.220
HCN...HCN	0.056	0.022	-0.066	0.035	-0.040	-0.008	0.329	-0.013	0.317
HNC...HNC	0.034	0.108	0.007	0.027	-0.034	-0.015	0.410	0.027	0.563
HCN...HF	0.021	0.218	-0.072	0.062	-0.056	-0.009	0.403	-0.017	0.550
HF...HCl	0.043	0.095	-0.027	0.042	-0.004	0.025	0.054	0.002	0.229
H ₂ O...HF	0.029	0.247	-0.059	0.079	-0.063	0.035	0.247	0.018	0.532

^a The letter “d” labelling some of the terms refers to donor monomers;

^b Differences on dimerization.

Table 8: Variations on hydrogen bonding for contributions from charge, charge flux (donor, charge transfer and acceptor) and polarization changes (donor and acceptor) as given by the QTAIM/CCFDF analysis of the polar tensor elements (e) associated with parallel dipole moment derivatives for displacements of the bridge hydrogen along the X-H axis from CCSD/cc-pVQZ-mod calculations.^a

Differences ^b	Δq_{Hd}	$\Delta \left(\sum_{i \in d} z_{iHd} \frac{\partial q_i}{\partial z_{Hd}} \right)$	$\Delta \left(\sum_{i \in a} z_{YHd} \frac{\partial q_i}{\partial z_{Hd}} \right)$	$\Delta \left(\sum_{i \in a} z_{iY} \frac{\partial q_i}{\partial z_{Hd}} \right)$	$\Delta \left(\sum_{i \in d} \frac{\partial m_{i,z}}{\partial z_{Hd}} \right)$	$\Delta \left(\sum_{i \in a} \frac{\partial m_{i,z}}{\partial z_{Hd}} \right)$	Tot
HF...HF	0.021	0.157	0.053	0.008	0.003	0.051	0.294
HCl...HCl	0.018	0.063	0.076	-0.005	0.032	0.036	0.220
HCN...HCN	0.056	0.128	0.066	0.092	-0.010	-0.015	0.317
HNC...HNC	0.034	0.205	0.191	0.128	0.022	-0.017	0.563
HCN...HF	0.021	0.218	0.148	0.183	0.005	-0.026	0.550
HF...HCl	0.043	0.095	0.020	0.007	0.039	0.027	0.229
H ₂ O...HF	0.029	0.247	0.127	0.061	0.015	0.053	0.532

^a The letters “a” and “d” labelling some of the terms refer to acceptor and donor monomers, respectively;

^b Differences on dimerization.

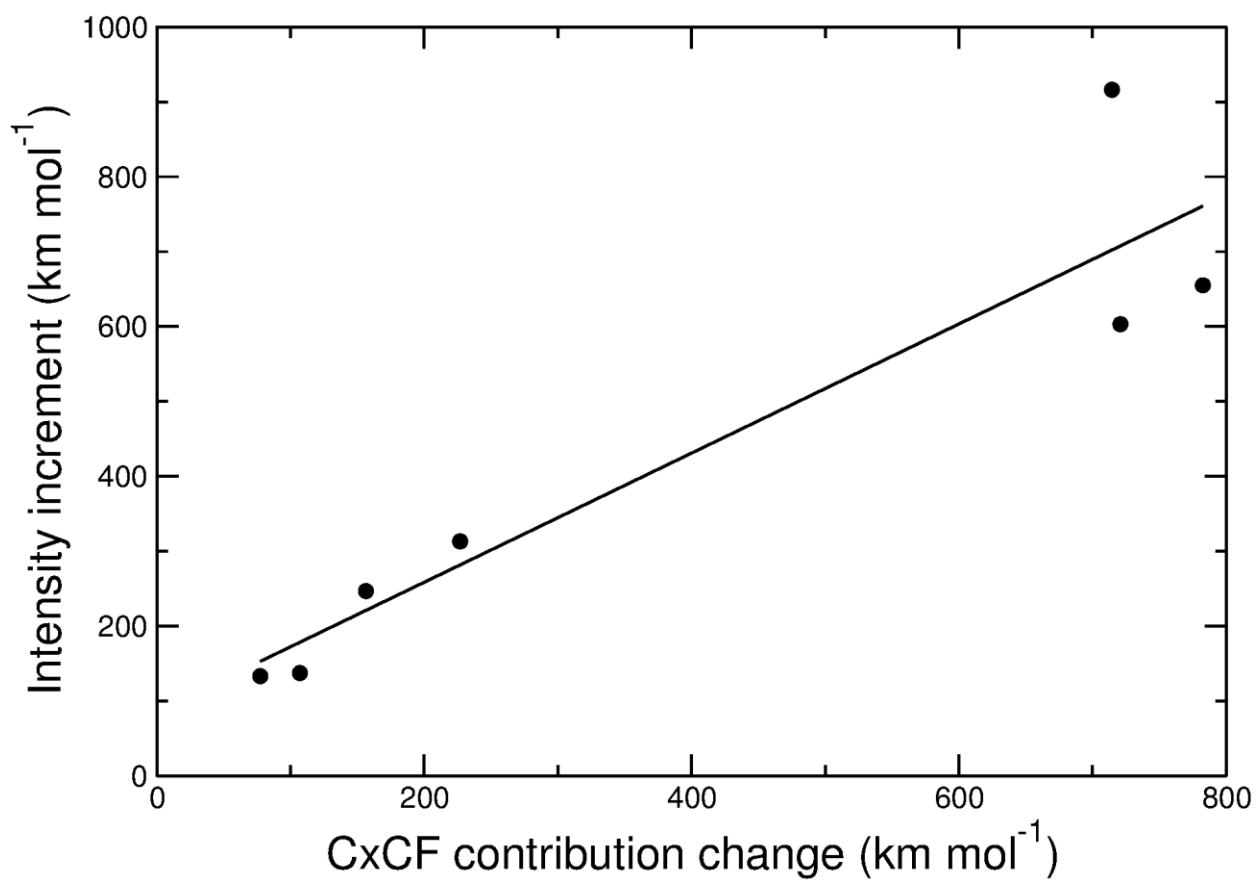


Figure 1: Infrared intensity enhancements of the HX_{donor} stretching mode on dimerization versus the corresponding changes in the charge – charge flux ($A_{\alpha}^{\text{C}\times\text{C}\text{F}}$) interaction.

References

- ¹ B.J. Howard, T.R. Dyke and W. Klemperer, *J. Chem. Phys.* 1984, **81**, 5417-5425.
- ² M.J. Elrod and R.J. Saykally, *J. Chem. Phys.* 1995, **103**, 933-949.
- ³ R.S. Ruoff, T. Emilsson, C. Chuang, T.D. Klots and H.S. Gutowsky, *Chem. Phys. Letters* 1987, **138**, 553-558.
- ⁴ A.C. Legon, D.J. Millen and S.C. Rogers, *Chem. Phys. Letters* 1976, **41**, 137-138.
- ⁵ K.C. Janda, J.M. Steed, S.E. and W. Klemperer, *J. Chem. Phys.* 1977, **67**, 5162-5172.
- ⁶ J.W. Bevan, Z. Kisiel, A.C. Legon, D.J. Millen and S.C. Rogers, *Proc. R. Soc. Lond. A* 1980, **372**, 441-451.
- ⁷ T.R. Dyke, B.J. Howard and W. Klemperer, *J. Chem. Phys.* 1972, **56**, 2442-2454.
- ⁸ K. Imura, T. Kasai, H. Ohoyama, H. Takahashi and R. Naaman, *Chem. Phys. Letters* 1996, **259**, 356-360.
- ⁹ E.J. Campbell and S.G. Kukolich, *Chem. Phys.* 1983, **76**, 225-229.
- ¹⁰ A.C. Legon, D.J. Millen and S.C. Rogers, *J. Mol. Spectrosc.* 1978, **70**, 209-215.
- ¹¹ Z. Kisiel, A.C. Legon and D.J. Millen, *J. Chem. Phys.* 1983, **78**, 2910-2914.
- ¹² A.S. Pine and B.J. Howard, *J. Chem. Phys.* 1986, **84**, 590-596.
- ¹³ L.W. Buxton, E.J. Campbell and W.H. Flygare, *Chem. Phys.* 1981, **56**, 399-406.
- ¹⁴ B.A. Wofford, M.E. Eliades, S.G. Lieb and J.W. Bevan, *J. Chem. Phys.* 1987, **87**, 5674-5680.
- ¹⁵ A.C. Legon, D.J. Millen, P.J. Mjöberg, and S.C. Rogers, *Chem. Phys. Letters* 1978, **55**, 157-159.
- ¹⁶ R.K. Thomas, *Proc. R. Soc. Lond. A* 1975, **344**, 579-592.
- ¹⁷ A.C. Legon, D.J. Millen and H.M. North, *Chem. Phys. Letters* 1987, **135**, 303-306.
- ¹⁸ C.L. Collins, K. Morihashi, Y. Yamaguchi and H.F. Schaefer III, *J. Chem. Phys.* 1995, **103**, 6051-6056.
- ¹⁹ N. Ohashi and A.S. Pine, *J. Chem. Phys.* 1984, **81**, 73-84.
- ²⁰ B.F. King and F. Weinhold, *J. Chem. Phys.* 1995, **103**, 333-347.
- ²¹ D.J. Nesbitt, *Chem. Rev.*, 1988, **88**, 843-870.
- ²² U. Dinur and A.T. Hagler, *J. Chem. Phys.* 1992, **97**, 9161-9172.
- ²³ B.A. Zilles and W.B. Person, *J. Chem. Phys.* 1983, **79**, 65-77.
- ²⁴ G.A. Yeo and T.A. Ford, *J. Mol. Struct.* 1992, **270**, 417-439.
- ²⁵ D.J. Swanton, G.B. Bacskay and N.S. Hush, *Chem. Phys.* 1983, **82**, 303-315.
- ²⁶ D. Galimberti, A. Milani, and C. Castiglioni, *J. Chem. Phys.* 2013, **139**, 074304.
- ²⁷ W.T. King and G.B. Mast, *J. Phys. Chem.* 1976, **80**, 2521-2525.
- ²⁸ M.M. Szczesniak, and S. Scheiner, *Chem. Phys. Lett.* 1986, **131**, 230-236.
- ²⁹ T.Q. Teodoro and R.L.A. Haiduke, *Comput. Theor. Chem.* 2013, **1005**, 58-67.
- ³⁰ V.H. Rusu, M.N. Ramos and R.L. Longo, *J. Mol. Struct.* 2011, **993**, 86-90.
- ³¹ R.L.A. Haiduke and R.E. Bruns, *J. Phys. Chem. A* 2005, **109**, 2680-2688.
- ³² R.F.W. Bader, *Acc. Chem. Res.* 1985, **18**, 9-15.
- ³³ R.F.W. Bader, *Atoms in Molecules: a Quantum Theory*; Clarendon Press: Oxford, 1990.
- ³⁴ R.F.W. Bader, A. Larouche, C. Gatti, M.T. Carrol, P.J. MacDougall and K.B. Wiberg, *J. Chem. Phys.* 1987, **87**, 1142-1152.
- ³⁵ T.W. Schmidt, T. Pino, P. Bréchnignac, *J. Phys. Chem. A* 2009, **113**, 3535-3541.

- ³⁶ R.L.A. Haiduke, H.P. Martins Filho, and A.B.F. da Silva, *Chem. Phys.*, 2008, **348**, 89-96.
- ³⁷ A.F. Silva, W.E. Richter, H.G.C. Meneses, S.H.D.M. Faria and R.E. Bruns, *J. Phys. Chem. A* 2012, **116**, 8238-8249.
- ³⁸ U. Koch, P.L.A. Popelier, *J. Phys. Chem.* 1995, **99**, 9747-9754.
- ³⁹ J.A. Platts, *Phys. Chem. Chem. Phys.* 2000, **2**, 3115-3120.
- ⁴⁰ M.T. Carroll, R.F.W. Bader, *Mol. Phys.* 1988, **65**, 695-722.
- ⁴¹ A.M. Pendás, M.A. Blanco, E. Francisco, *J. Chem. Phys.* 2006, **125**, 184112.
- ⁴² M.J. Frisch, G.W. Trucks, H.B. Schlegel, G.E. Scuseria, M.A. Robb, J.R. Cheeseman, J.A. Montgomery Jr., T. Vreven, K.N. Kudin, J.C. Burant, J.M. Millam, S.S. Iyengar, J. Tomasi, V. Barone, B. Mennucci, M. Cossi, G. Scalmani, N. Rega, G.A. Petersson, H. Nakatsuji, M. Hada, M. Ehara, K. Toyota, R. Fukuda, J. Hasegawa, M. Ishida, T. Nakajima, Y. Honda, O. Kitao, H. Nakai, M. Klene, X. Li, J.E. Knox, H.P. Hratchian, J.B. Cross, V. Bakken, C. Adamo, J. Jaramillo, R. Gomperts, R.E. Stratmann, O. Yazyev, A.J. Austin, R. Cammi, C. Pomelli, J.W. Ochterski, P.Y. Ayala, K. Morokuma, G.A. Voth, P. Salvador, J.J. Dannenberg, V.G. Zakrzewski, S. Dapprich, A.D. Daniels, M.C. Strain, O. Farkas, D.K. Malick, A.D. Rabuck, K. Raghavachari, J.B. Foresman, J.V. Ortiz, Q. Cui, A.G. Baboul, S. Clifford, J. Cioslowski, B.B. Stefanov, G. Liu, A. Liashenko, P. Piskorz, I. Komaromi, R.L. Martin, D.J. Fox, T. Keith, M.A. Al-Laham, C.Y. Peng, A. Nanayakkara, M. Challacombe, P.M.W. Gill, B. Johnson, W. Chen, M.W. Wong, C. Gonzalez and J.A. Pople, GAUSSIAN 03, Revision D.02, Gaussian Inc., Wallingford, CT, 2004.
- ⁴³ S. J. Yao and J. Overend, *Spectrochim. Acta A*, 1976, **32**, 1059-1065.
- ⁴⁴ T.H. Dunning Jr, *J. Chem. Phys.* 1989, **90**, 1007-1023.
- ⁴⁵ D.E. Woon, and T.H. Dunning Jr, *J. Chem. Phys.* 1993, **98**, 1358-1371.
- ⁴⁶ AIMAll (Version 12.08.21), T. A. Keith, TK Gristmill Software, Overland Park KS, USA, 2012 (aim.tkgristmill.com).
- ⁴⁷ C.F. Matta and R.J. Boyd, Eds. *The Quantum Theory of Atoms in Molecules: From Solid State to DNA and Drug Design*; Wiley-VCH: Weinheim, 2007.
- ⁴⁸ S.F. Boys and F. Bernardi, *Mol. Phys.* 1970, **19**, 553-566.
- ⁴⁹ S. Simon, M. Duran and J.J. Dannenberg, *J. Chem. Phys.* 1996, **105**, 11024-11031.
- ⁵⁰ W.M. Haynes, Ed. *CRC Handbook of Chemistry and Physics*; 93rd Ed. (Internet Version 2013); CRC Press/Taylor and Francis, Boca Raton, FL.
- ⁵¹ T. Okabayashi and M. Tanimoto, *J. Chem. Phys.* 1993, **99**, 3268-3271.
- ⁵² A.E. Reed, L.A. Curtiss and F. Weinhold, *Chem. Rev.* 1988, **88**, 899-926.
- ⁵³ J.B. Burkholder, A. Sinha, P.D. Hammer and C.J. Howard, *J. Mol. Spectrosc.* 1987, **126**, 72-77.
- ⁵⁴ D.M. Bishop and L.M. Cheung, *J. Phys. Chem. Ref. Data* 1982, **11**, 119-133.
- ⁵⁵ R.M. Vichiatti and R.L.A. Haiduke, *Spectrochim. Acta A* 2013, **114**, 197-204.
- ⁵⁶ A.S. Pine, W.J. Lafferty and B.J. Howard, *J. Chem. Phys.* 1984, **81**, 2939-2950.
- ⁵⁷ R.F. Bader and C.F. Matta, *J. Phys. Chem. A* 2004, **108**, 8385-8394.
- ⁵⁸ A.F. da Silva Filho, W.E. Richter, L.A. Terrabuio, R.L.A. Haiduke and R.E. Bruns, *J. Chem. Phys.* 2014, **140**, 084306.